Nigerian Journal of Applied Physics (NJAP)
ISSN Print: XXXX-XXXX
ISSN Online : XXXX-XXX
DOI: https://doi.org/10.62292/njap-v1i1-2025-2
Volume 1(1), September 2025

Investigation of X-Ray Shielding Properties of Concretes Made with Cassava Flour, Sawdust and Charcoal

***Odoh, Christopher Mmaduabuchi, Onudibia, Moses Ejike, Ifeanyi, Chukwuebuka, Ezekiel, Yangde Andekwe, Osimiri, Olisa Leonard and Alfred, Rimamsiwe**

Department of Pure and Applied Physics, Federal University Wukari, Taraba State, Nigeria.

*Corresponding author's email: odohchristopher@fuwukari.edu.ng
ORCID iD: https://orcid.org/0000-0002-2872-8744

ABSTRACT

In this study, we fabricated concretes with cassava flour, sawdust and charcoal collected from Baissa, Kurmi Local Government Area, Taraba State, Nigeria. These composites were investigated on their abilities to shield x-ray reference qualities; 40 kV, 80 kV, and 120 kV at the radiology department of Jos University Teaching Hospital, Jos, Plateau State Nigeria, using a RAD 12 X-ray machine. The incident and the transmitted radiation dose were used to estimate the linear attenuation, mass attenuation and half value thickness of each composite shield. The transmitted photon intensities at 80 kVp and 120 kVp were then compared with the densities of the various sample blocks to investigate the effect of density on their shielding abilities. Pearson Correlation revealed that densities were negatively related to the transmitted photon intensities at 80 kVp and 120 kVp, with coefficients of [r(10) = -.589,p = .05] and [r(10) = -.925,p =.01] respectively. However, a high density obtained in the charcoal composite and a low mechanical strength observed in the cassava composite made the two aggregates unfit for x-ray shielding purposes where density is an important factor to be considered. The average densities and half value thickness (HVT) of the sawdust composite were compared with the densities and HVT of Lead and Concrete. A scatter plot analysis was used to generate model equations and estimate the Lead and concrete equivalent densities. The results show that lead shields can be replaced with the sawdust composite to shield against 80 kVp and 120 kVp x-ray sources at reduced densities of 66.5% and 52.5% respectively. Concrete shields can also be replaced with the sawdust composite in shielding against 80 kVp and 120 kVp x-ray sources at a reduced density of 7.2% and 4.94% respectively. This is a strong indication that sawdust composite can be very efficient in x-ray shielding applications, such as in mobile x-ray sources.

Keywords:
Cassava flour,
Sawdust,
Charcoal,
Linear attenuation,
Mass attenuation,
Half value thickness.

INTRODUCTION

Since ionizing radiations can have serious negative health impacts, radiation shielding is important for both environmental and human safety (Aggrey-Smith et al., 2016). One of the best radiation protection strategies is radiation shielding, along with reducing exposure duration and removing oneself from the source (Mahdy et al., 2002).

Any physical barrier intended to offer defence against ionizing radiation is known as a radiation shield. Theoretically, radiation can be safely attenuated using any material. Concrete and lead are more widely used for this purpose, because of their specific qualities (Aggrey-Smith et al., 2016). While choosing a material for radiation shielding purposes, the following must be taken into account: desired reduced radiation levels, ease of heat dissipation, resistance to radiation damage, necessary thickness and weight, permanence of shielding, and availability of the material (Wilkinson, 2004). According to Mahdy et al. (2002), a suitable shielding material should have a high photon attenuation coefficient so that a little thickness will result in a considerable drop in intensity.

Heavy metals like lead and tungsten are perfect for shielding because of their high densities (Erdem et al., 2010). But using such materials to develop and construct radiation shields have shown to be highly challenging (Kenneth, 2015), and lead compounds have been shown to be extremely poisonous and can cause lead poisoning (Akkurt et al., 2006). Although concrete

materials have been shown to be more effective and non-toxic, their application in radiation shield construction remains problematic due to their heavy masses and the space needed for such structures (El-Khayatt et al., 2013). As a result, research into more effective materials continues.

Many theoretical and experimental studies have been carried out in the literature to create new heavy concrete. Heavy concrete has been made from several minerals, such as limonite and siderite, to offer protection from gamma and neutron radiations (Akkurt et al., 2010; Sahadath et al., 2015). Using aggregates like calcium (Ca), strontium (Sr), barium (Ba), radium (Ra), and magnesium (Mg), Seltborg et al. (2005) to make heavy concretes that may be utilized to protect gamma and neutron radiations from nuclear reactors can be more efficient, but their cost and limited supply make them unfeasible for shielding applications (Schaeffer, 1973).

Photons traveling in a straight line make up a photon beam. The photon beam's intensity decreasing as it travels through a substance is known as attenuation. The rate at which a particular photon beam attenuates as it travels through a substance is determined by the total linear attenuation coefficient (Godwin et al., 2017). It depends on the type of material and the photon energy, and it is mathematically expressed by equation (1):

$$\mu_t = \frac{1}{x} ln \frac{I_0}{I} \quad (1)$$

where; I_0 is the intensity of the photon beam just before it enters the material, and I is its intensity at a depth(x). The unit of linear attenuation coefficient is cm^{-1}.

A material's mass attenuation coefficient, also known as its mass narrow beam attenuation coefficient, describes how readily a photon beam can travel through its volume. It is mathematically expressed in equation (2):

$$\mu_m = \frac{\mu_t}{\rho} \quad (2)$$

where; ρ is the density of the material. The unit of mass attenuation coefficient is cm^2/g.

The thickness of a homogeneous absorber that reduces the narrow beam intensity I_0 to half (50%) of its initial intensity is known as the half-value layer (HVL) (Podgorsak, 2005). Since at half value thickness, the intensity reduces to half of its initial value $(\frac{1}{2} I_0)$, substituting this in equation (1), gives equation (3) and rearranging gives equation (4):

$$\frac{1}{2} I_0 = I_0 e^{-\mu_t x} \quad (3)$$

$$x = HVL = \frac{ln2}{\mu_t} \quad (4)$$

where; HVL is the half value layer.

MATERIALS AND METHODS

Study Area

Baissa, Kurmi Local Government Area, Taraba State, North-Eastern Nigeria is where all of the local aggregates used in this study were obtained and processed. The materials are in large abundance in this geographic area.

Aggregates

In this investigation, sawdust, charcoal, and cassava flour were used as aggregates. Only the sawing of mahogany wood produced the sawdust. Large agglomerate particles were removed from the sawdust after it was dried for a week at 31 to 32 ºC. This made the dust more uniform and ensured that the aggregate and cement were properly mixed. The dried, burned mahogany wood was used to make the charcoal. Since mahogany is the most common wood species in that region, it was selected. To guarantee sufficient mixing with the other shield aggregates, the charcoal was ground into a powder using a mortar and pestle. Cassava tubers that were prepared locally were used to make cassava flour. The peeled cassava tubers were from a farm in the research area. The peeled cassavas were dried at temperatures between 31 – 32ºC for 7 days. After 7 days, the cassava tubers were crushed and grinded into powder to obtain cassava flour. Masses of the sawdust, charcoal, cassava flour, white sand, cement and gravel were measured using an SF-400 electronic weighing balance (± 0.1 g), and volume determined by water displacement method using a calibrated measuring cylinder of 200 ml. The density of each material was estimated using equation (5):

$$\rho = \frac{m}{v} \left(\frac{g}{cm^3}\right) \quad (5)$$

where; ρ, m and v represent the density, mass and volume, respectively.

Mix Design and Moulding

The mix ratios that would achieve the highest compressive strength to make the combination more appropriate for radiation protection were chosen as 1:1:1, 1:1:2, and 1:1:3 (cement to gravel to aggregate). The aggregates were combined with sharp sand, stone pebbles (gravels), and Dangote 3X cement by volume replacement of the aggregates. To make the mixture workable, clean tap water was added, and it was then moulded into blocks that were 15 cm by 15 cm by 2 cm shown in Figure 1. From each aggregate, three block samples (A, B, and C, which stand for 1:1:1, 1:1:2, and 1:1:3, respectively) were made, making them a total of twelve block samples. The moulded samples were allowed to dry in a controlled setting at room temperature and atmospheric pressure. The drying process entailed wetting daily with water for another 14 days making a total of 21 days.

Figure 1: Blocks drying in ambient conditions

Density Measurement

The mass of the prepared samples was measured using a digital weighing balance. The volume of the samples was determined from the product of the length, width and height dimensions measured with a Vernier caliper (i.e 15 x 15 x 2 = 450 cm^3). Moreover, the density was then estimated using equation (5).

Determining Transmission Parameters

In the radiology department of Jos University Teaching Hospital, the narrow beam technique was used to conduct an experiment to ascertain the blocks' transmission properties. The experimental setup was as shown in Figure 2.

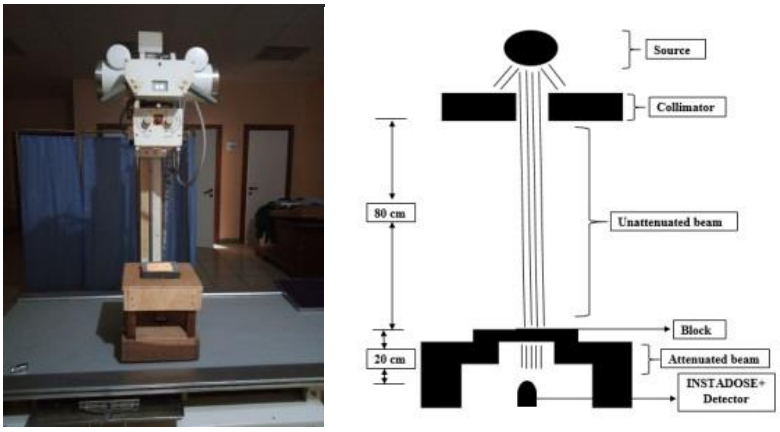

Figure 2: Experimental Setup

A RAD 12 X-ray machine (model: 222660, Serial Number: 47476HL7) and an INSTADOSE+ radiation detector (model: IDPLUS, Serial Number: 20201008), which work with a software (INSTADOSE Companion Application), to give instantaneous radiation dosage in milli Siverts (mSv), were used in the experiment. The INSTADOSE+ detector was placed 100 cm away from the collimator of the x-ray tube. With the guidance of the collimator light, an x-ray field was collimated to 10 cm x 10 cm to ensure coverage of the sensitive window of the detector. On the control panel, values of 40 kVp and 50 mAs were adjusted in order to ascertain the tube output behaviour and initial radiation dosage I_0 in milli Sivert (mSv). The INSTADOSE+ detector was used to measure the tube output after an exposure. At 50 mAs, this step was repeated at potentials of 40 kVp, 80 kVp, and 120 kVp. In order to calculate the transmitted dose, I in milli Siverts (mSv), the block sample was then positioned 20 cm from the INSTADOSE+ radiation detector and 80 cm from the x-ray tube's collimator. A second exposure was then made. This procedure was repeated for the remaining 11 samples making a total of 36 exposures. The initial dose intensity I_0(mSv) and the final intensity I(mSv) obtained were used to determine the linear attenuation coefficient(μ_l), mass attenuation coefficient (μ_m) and the half value thickness (HVT) using equations 1.1, 1.2 and 1.3 respectively. The effect of density on the shielding abilities of the various composite shields was analyzed using the Pearson Correlation and Scatter Plot statistical tools

RESULTS AND DISCUSSION

The experiments generated the dosage intensity results. Before analysing the samples, without the samples on the detector, the initial dose intensities for I_0(40) at 40 kVp, I_0(80) at 80 kVp, and I_0(120) at 120 kVp were determined at a constant tube current of 50 mAs. The values for the different voltages were found to be 0.1 mSv, 0.26 mSv, and 0.71 mSv for I_0(40), I_0(80), and I_0(120), respectively. Table 1 displays the attenuated photo intensity for each of the samples analysed.

The half value layer, the mass attenuation coefficient (μ_m), and the linear attenuation coefficient (μ_t), computed using the results of Table 1 are summarized in Table 2.

Table 1: Final Dose Intensities in Msv

S/N	Aggregates	Sample ID	Densities (g/cm^3)	Final Photo Intensities I (mSv) at Various Tube Voltages		
				40 kVp ($I_{0(40)}$=0.1 mSv)	80kVp $I_{0(80)}$=0.26 mSv	120kVp $I_{0(120)}$=0.71 mSv
1.	Sharp Sand	A	2.72	<0.03	0.08	0.13
2.		B	2.68	<0.03	0.06	0.05
3.		C	2.49	<0.03	0.06	0.11
4.	Sawdust	A	1.96	<0.03	0.06	0.22
5.		B	1.58	<0.03	0.07	0.27
6.		C	1.23	<0.03	0.09	0.27
7.	Charcoal	A	1.86	<0.03	0.07	0.22
8.		B	1.76	<0.03	0.08	0.25

9.		C	1.57	0.06	0.09	0.27
10.	Cassava	A	1.73	<0.03	0.07	0.22
11.		B	1.53	<0.03	0.08	0.22
12.		C	1.44	0.05	0.08	0.25

Table 2: The Half-Valued Layer, Linear and Mass Attenuation Coefficients of Various Block Samples

S/N	Aggregates	Sample ID	Attenuation Parameters								
			40 kVp			80kVp			120kVp		
			μ_t (cm^{-1})	μ_m (cm^2/g)	HVL (cm)	μ_t (cm^{-1})	μ_m (cm^2/g)	HVL (cm)	μ_t (cm^{-1})	μ_m (cm^2/g)	HVL (cm)
1.	Sharp	A	<0.60	<0.221	<1.15	0.59	0.217	0.82	0.85	0.312	1.18
2.	Sand	B	<0.60	<0.225	<1.15	0.73	0.274	0.52	1.33	0.495	0.95
3.		C	<0.60	<0.242	<1.15	0.73	0.294	0.74	0.93	0.375	0.95
4.	Sawdust	A	<0.60	<0.307	<1.15	0.73	0.374	0.95	0.59	0.299	1.18
5.		B	<0.60	<0.381	<1.15	0.66	0.415	1.06	0.48	0.306	1.43
6.		C	<0.60	<0.489	<1.15	0.53	0.431	1.31	0.48	0.393	1.43
7.	Charcoal	A	<0.60	<0.324	<1.15	0.66	0.353	1.06	0.59	0.315	1.18
8.		B	<0.60	<0.342	<1.15	0.59	0.335	1.18	0.52	0.297	1.33
9.		C	0.26	0.163	2.71	0.53	0.338	1.31	0.48	0.308	1.43
10.	Cassava	A	<0.60	<0.348	<1.15	0.66	0.379	1.06	0.59	0.339	1.18
11.		B	<0.60	<0.394	<1.15	0.59	0.385	1.18	0.59	0.383	1.18
12.		C	0.35	0.241	2.00	0.59	0.409	1.18	0.52	0.362	1.33

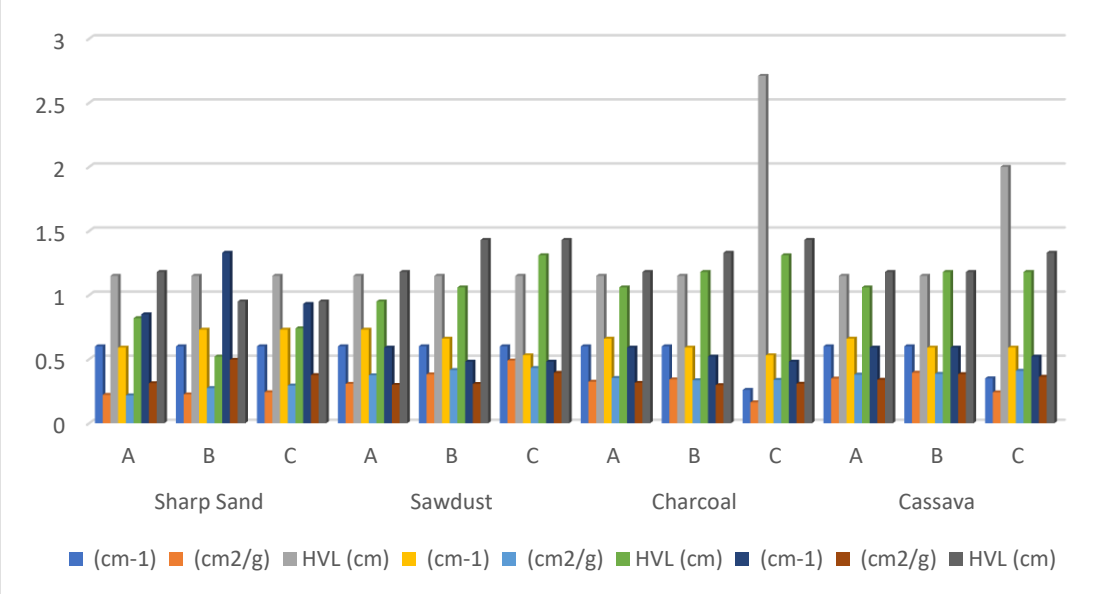

Figure 3: Comparing the linear attenuation, mass attenuation and half value thickness of the various block samples at the various tube voltages

Table 2 shows the mass attenuation and linear coefficients for the twelve (12) samples analysed, while Figure 3 compares the HVL, linear and mass attenuation coefficients composites with the control composites. Figure 3 shows that samples with sample IDs Control B, Control C, and Sawdust A had the highest linear attenuation coefficients of 0.73 cm^{-1} at 80 kVp. However, Sawdust C and Charcoal C, had the lowest linear attenuation coefficients of 0.53 cm^{-1} at 80 kVp. The maximum linear attenuation coefficient of 1.33 cm^{-1} at 120 kVp was obseverd in control sample B, while the lowest linear attenuation coefficients of 0.48 cm^{-1} was found in sawdust samples B and C. In the 80 kVp voltage range, the samples linear attenuation coefficients were 0.20 cm^{-1}, whereas in the 120 kVp voltage range, it was 0.85 cm^{-1}.

Figure 3 shows that at the 80 kVp tube voltage, Sawdust C and Control A had the highest and lowest mass attenuation coefficients of 0.43 cm^2/g and 0.22 cm^2/g, respectively. While at 120 kVp tube voltage, control sample B and sawdust sample B had the highest and lowest mass attenuation coefficients of 0.50 cm^2/g and 0.30 cm^2/g, respectively. Figure 3 also shows that the samples transmitted photon intensities at 40 kVp tube voltage were less than 0.03 mSv, which corresponds to a linear attenuation coefficient of less than 0.60 cm^{-1}. However, Charcoal Sample C and Cassava Sample C displayed transmitted photon intensities of 0.06 mSv

and 0.05 mSv, respectively at linear attenuation coefficients of 0.26 cm^{-1} and 0.35 cm^{-1} respectively.
The results of a Pearson product moment correlation performed to examine the connection between the transmitted photon intensities at 80 kVp and 120 kVp and the densities of composite shields were shown in Table 3. The findings revealed that the density was inversely related with transmitted photon intensities at 80 kVp as r(10) = -.589 at a significance level of 0.044, as illustrated in Table 3 and Figure 4, and at 120 kVp, r(10) = -.925 at a significant level of 0.000 as illustrated in Table 3 and Figure 5. This indicates that as densities increased, the transmitted photon intensity decreased. Similar results have been reported by (Akkurt et al., 2010; Abdo, 2002; Erdem et al., 2010; Mortazavi et al., 2010) in similar investigations.

Table 3: Showing the Correlation Between the Density of Composite Shields in Gcm^{-3} and the Transmitted Photon Intensities at 80 Kvp and 120 Kvp Tube Voltages

		Transmitted Photon Intensities at 80 kVp	Transmitted Photon Intensities at 120 kVp
Density (g/cm^3)	Pearson Correlation	-0.589*	-0.925**
	Sig. (2-tailed)	.044	.000
	N	12	12

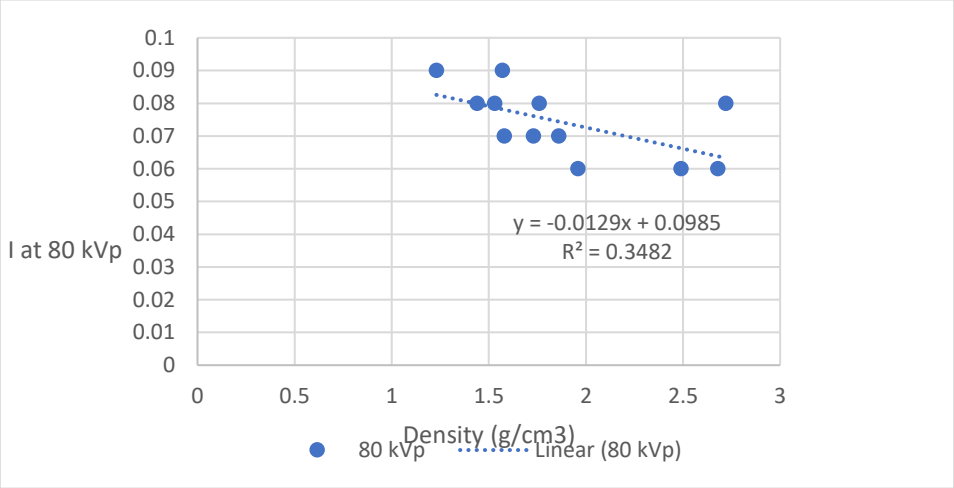

Figure 4: Scatter Plots of Transmitted Photon Intensity Against Densities of Shields At 80 Kvp

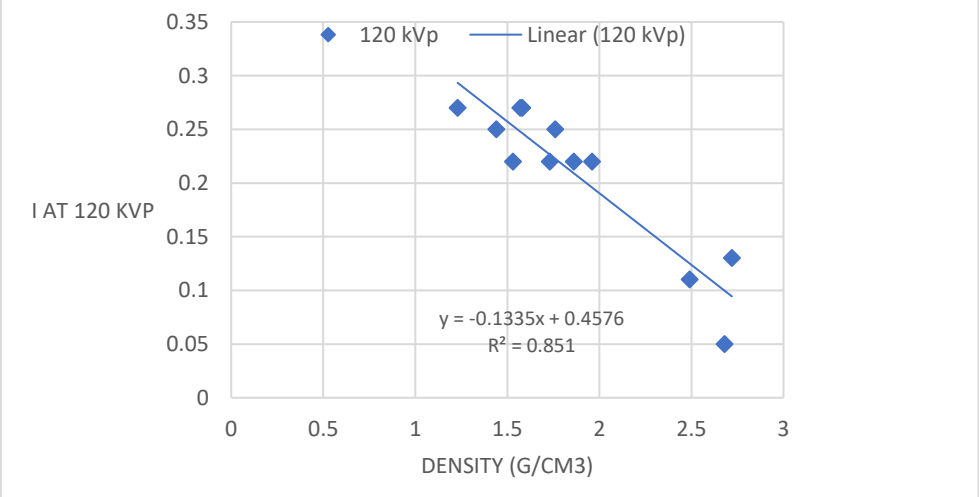

Figure 5: Scatter Plots of Transmitted Photon Intensity Against Densities of Shields at 120 kVp

The average values of densities and half value thicknesses of each of the aggregate analysed was compared with those of lead (Pb) and concrete in Table 4. Since lead (Pb) and concrete are the most widely used as radiation shields, they were chosen as references in this study. At 80 kVp and 120 kVp, sawdust and cassava aggregates show low HVT of 1.11 cm and 1.14 cm, and 1.35 cm and 1.23 cm, respectively, with average densities of 1.59 g/cm^3 and 1.57 g/cm^3, respectively. Also, Table 4 shows that the charcoal aggregate has the maximum density (1.73 g/cm^3) and HVT of 1.18 and 1.31 cm at 80 kVp and 120 kVp, respectively. The poor performance of charcoal aggregates in shielding x-rays despite having higher

average density than the sawdust and cassava aggregates, could be attributed to the porous nature of charcoal.

When compared the HVT of the two best-performing aggregates (sawdust and cassava) with those of lead (Pb) and concrete, it was found that the half value thickness of lead (density = 11.34 g/cm^3) was 0.024 cm (NIST, 2004), which is slightly less than 46 times that of the sawdust aggregate at 80 kVp, and 0.028 cm (NIST, 2004), which is slightly less than 48 times that of sawdust at 120 kVp. Also, at 80 kVp and 120 kVp, respectively, the half value thicknesses of the cassava aggregates were similarly found to be about 46 and 44 times smaller than those of lead. While the density of lead was found to be almost seven times that of the sawdust and cassava composite shields. Also, the half value thicknesses of the concrete shields used as the control experiment, sawdust and cassava aggregates were compared (Table 4). It was found that at 80 kVp and 120 kVp, the half value thicknesses of the Cassava and Sawdust composite shields were slightly above 1.6 and 1.2 times, respectively that of the control samples, whereas the control samples densities were about 1.6 times greater than those of the Cassava and Sawdust composite shields.

However, the cassava composite shields show lower mechanical strength in comparison to other composite shields. This was as a result of the cassava aggregate was unable to properly bind with the cement.

Table 4: Comparing the Average Densities and half value layer for each aggregate with the density and half value thickness of Lead and Concrete

Aggregates	Average Density (g/cm^3)	Average HVL at 80 kVp (cm)	Average HVL at 120 kVp (cm)
Sawdust	1.59	1.11	1.35
Charcoal	1.73	1.18	1.31
Cassava	1.57	1.14	1.23
Concrete (Control)	2.63	0.69	1.03
Lead (Pb) (NIST, 2004).	11.34	0.024	0.028

The plots of half value thicknesses of the sawdust composites shield against their densities were shown in Figures 6 and 7, which show the model equations that approximated the Lead and Concrete equivalents of the best-performing composite shield. The lead and concrete equivalents of the sawdust composite shields were estimated using the model equations from the graphs were presented in Table 5. The findings indicate that at 80 kVp and 120 kVp x-ray sources, sawdust composite shields can be used in place of lead shields at reduced densities of 66.5% and 52.5%, respectively, while concrete shields can be replaced with sawdust composites at reduced densities of 7.2% and 4.94%, respectively.

Table 5: Concrete and Lead Equivalent Densities for Sawdust Composite Shields

KVp	Concrete Equivalent Density (g/cm^3)	Lead Equivalent Density (g/cm^3)
80	2.44	3.80
120	2.50	5.39

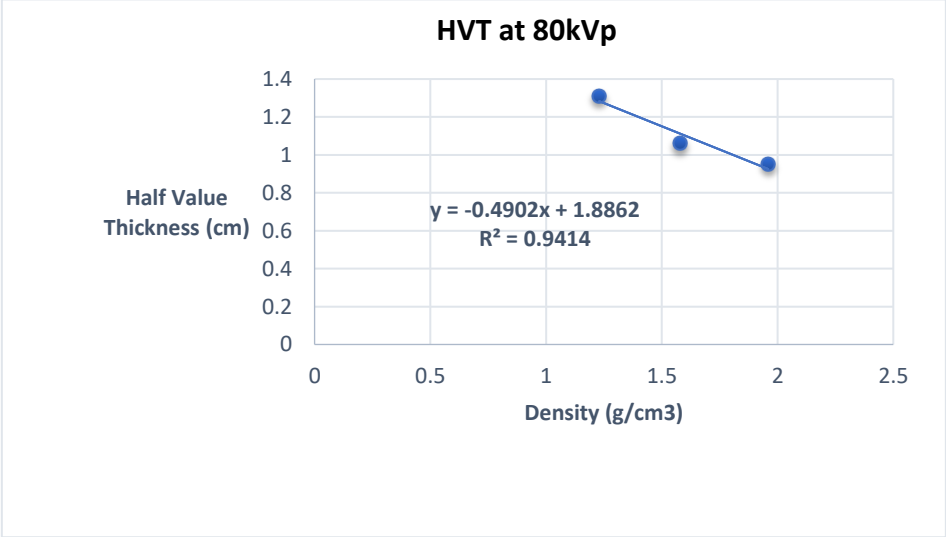

Figure 6: Graph of Half Value Thickness of Sawdust Composite Shields Against Density at 80 kVp

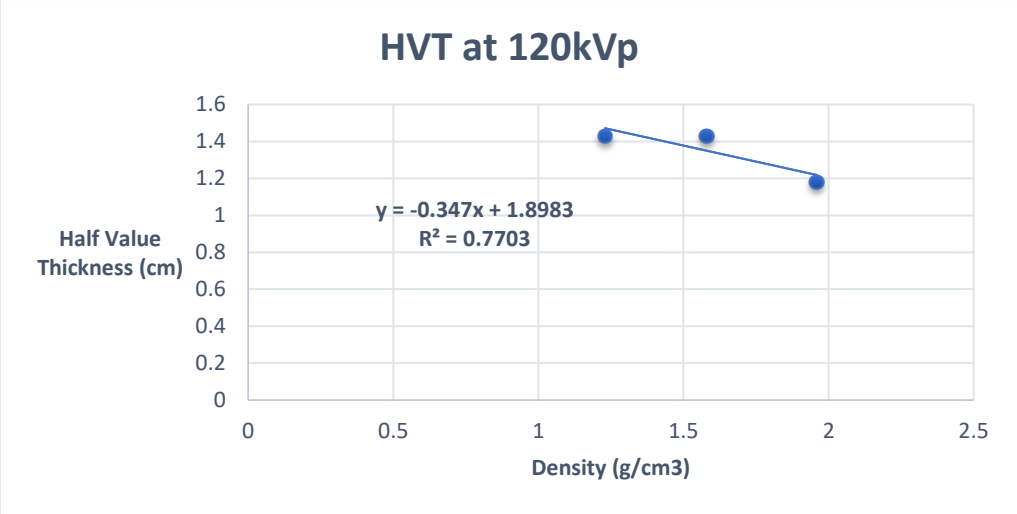

Figure 7: Graph of Half value thickness of Sawdust Composite shields against density at 120 kVp

In radiation shielding applications where density is an important consideration, like in mobile x-ray sources, this is a clear sign that sawdust composites will work well. Also, comparing the pricing and availability of lead and sawdust composite shields, the sawdust is more readily available locally, whereas lead is more costly and scarce. Due to their availability and low cost, sawdust composites are more cost-effective than lead shields. As of November, 2024, 1 kg of lead costs 1.5 USD (2,498.73 NGN), according to dailymetalprice.com. The cost of one pound of the sawdust composite shields used in this investigation was less than 500.00 NGN.

CONCLUSION

The findings of this study showed that sawdust composite as a preferable option for x-ray shielding in mobile x-ray sources, since they can provide an equivalent shielding to concrete at a reduced density of more than 50%. Also, sawdust composites are more affordable and easily accessible that can offer comparable shielding ability like lead at a lower density. For x-ray mobile installations, sawdust composites shields can be a superior shielding candidate for x-ray sources.

REFERENCES

Abdo, A. E. (2002). "Calculation of the Cross-Sections for Fast Neutrons and Gamma-Rays in Concrete Shields" *Annals of Nuclear Energy.* 29(16): 1977–1988. https://doi.org/10.1016/S0306-4549(02)00019-1

Aggrey-Smith, S., Preko, K., Owusu F. W., and Amoako J. K. (2016). "Study of Radiation Shielding Properties of Selected Tropical Wood Species for X-Rays in the 50-150kev Range" *The Open Access Journal of Science and Technology.* 4(2): 101-105. https://doi.org/10.11131/2016/101150

Akkurt, I., Basyigit, C., Kilincarslan, S., Mavi, B., and Akkurt, A. (2006). "Radiation Shielding of Concretes Containing Different Aggregates Cement and Concrete Composites". *Annals of Nuclear Energy*. 28(3): 153-157. https://doi.org/10.1016/j.cemconcomp.2005.09.006

Erdem, M., Baykara, O., Doğru, M., and Kulu F. A. (2010). "Novel Shielding Material Prepared from Solid Waste Containing Lead for Gamma Ray" *Radiation Physics and Chemistry*. 9(1): 917–922. https://doi.org/10.1016/j.radphyschem.2010.04.009

El-Khayatt, A. M., and Akkurt, I. (2013). "Photon Interaction, Energy Absorption and Neutron Removal Cross Section of Concrete Including Marble" *Annals of Nuclear Energy.* 60(12): 8-14. https://doi.org/10.1016/j.anucene.2013.04.021

Godwin B. E., James A. A., Oludotun O. F. (2017). "Attenuation Characteristic of Clay Irradiated with X-Ray in the Range between 40 Kev and 120 Kev*". IOSR Journal of Applied Physics*. ISSN: 2278-4861.Volume 9, Issue 6 Ver. IV. Doi: 10.9790/4861-0906043947 www.iosrjournals.org

Kenneth, J. S., and Richard, E. F. (2015). Radiation Shielding Technology. *Journal of Physics:* 611(2): 21-27. https://doi.org/10.1097/01.HP.0000148615.73825.b1

Mahdy, M., Speare, P. R. S., and Abdel-Reheem, A. H. (2002). Effect of Transient High Temperature on Heavyweight, High Strength Concrete. 15th A. S. C. E Engineering Mechanics Conference, June 2-5. New York: University Of Columbia.

Mortazavi, S. M. J., Mosleh-Shirazi, M. A., Baradaran G. M., Siavashpour, Z., Farshadi, A., Ghafoori, M., and Shahvar, A. (2010). Production of a Datolite-Based Heavy Concrete for Shielding Nuclear Reactors and Megavoltage Radiotherapy Rooms. *Iranian Journal of Radiation Research.* 8(1): 11–15.

National Institute of Standards and Technology (NIST). (2004). "Tables Of X-Ray Mass Attenuation Coefficient and Mass Energy Absorption Coefficients from 1KeV to 20MeV for Elements Z=1 to 92 And 48 Additional Substances of Dosimetric Interest". *NIST Reference Database 126.*

Podgorsak E.B. (2005). "Radiation Oncology Physics: A Handbook for Teachers and Students". *IAEA Library Cataloguing in Publication Data— Vienna*. STI/PUB/1196 ISBN 92–0–107304. https://www-pub.iaea.org

Sahadath, H., Mollah, A. S., Kabir, K. A., and Huq, F. (2015). "Calculation of the Different Shielding Properties of Locally Developed Ilmenite-Magnetite (I-M) Concrete".*Journalon Radioprotection.* 50(3): 203-207. https://doi.org/10.1051/radiopro/2015005

Schaeffer, M. (1973). "Reactor Shielding for Nuclear Engineers.Division of Reactor Development and Technology U. S. Atomic Energy Commission" .p. 12. ISBN 0-87079-004-8. https://doi.org/10.2172/4479460

Seltborg, P., Polanski, A., Petrochenkov, S., Lopatkin, A., Gudowski, W., and Shvetsov, V. (2005). "Radiation Shielding of High-Energy Neutrons in SAD". *Nuclear Instruments and Methods in Physics Research.* 550(2): 313–328. https://doi.org/10.1016/j.nima.2005.04.071

Wilkinson, W. L. (2004). 'Relevance of IAEA Tests to Severe Accidents in Nuclear Fuel Cycle Transport". World Nuclear Transport Institute, London, UK 14th International Symposium on The Packaging Transportation of Radioactive Materials (PATRAM2004), Berlin, Germany. http://www.dailymetalprice.com/metalprices.php.